Emergent Bloch excitations in Mott matter

Nicola Lanatà, Tsung-Han Lee, Yong-Xin Yao, and Vladimir Dobrosavljević

Phys. Rev. B **96**, 195126 — Published 14 November 2017

DOI: 10.1103/PhysRevB.96.195126

Emergent Bloch Excitations in Mott Matter

Nicola Lanatà,[1] Tsung-Han Lee,[1] Yong-Xin Yao,[2] and Vladimir Dobrosavljević[1]

[1] *Department of Physics and National High Magnetic Field Laboratory, Florida State University, Tallahassee, Florida 32306, USA*

[2] *Ames Laboratory-U.S. DOE and Department of Physics and Astronomy, Iowa State University, Ames, Iowa IA 50011, USA*

We develop a unified theoretical picture for excitations in Mott systems, portraying both the heavy quasiparticle excitations and the Hubbard bands as features of an emergent Fermi liquid state formed in an extended Hilbert space, which is non-perturbatively connected to the physical system. This observation sheds light on the fact that even the incoherent excitations in strongly correlated matter often display a well defined Bloch character, with pronounced momentum dispersion. Furthermore, it indicates that the Mott point can be viewed as a topological transition, where the number of distinct dispersing bands displays a sudden change at the critical point. Our results, obtained from an appropriate variational principle, display also remarkable quantitative accuracy. This opens an exciting avenue for fast realistic modeling of strongly correlated materials.

PACS numbers: 71.27.+a, 71.30.+h,71.10.Hf

Introduction:— The physical nature of the excited states in strongly interacting quantum systems has long been a subject of much controversy and debate. Deeper understanding was achieved by Landau, more than half a century ago[1], who realized that in systems of fermions the Pauli principle provides a spectacular simplification. He showed that many properties of Fermi systems can be understood in terms of weakly interacting *quasiparticles* (QP), allowing a precise and detailed description of strongly correlated matter. Modern experiments provide for even more direct evidence of such QP excitations, for example from using angle-resolved photoemission spectroscopy (ARPES)[2] or scanning-tunneling microscopy (STM) methods[3].

The Fermi liquid paradigm, however, describes only the low energy excitations. At higher energies, the physical properties are often dominated by incoherent processes, which do not conform to the Landau picture. The task to provide a simple and robust theoretical description of such incoherent excitations has therefore emerged as a central challenge of contemporary physics. An intriguing apparent paradox is most evident around the Mott point. Here, ARPES and STM experiments provide often clear evidence of additional well-defined high energy excitations (Hubbard bands) which, while being fairly incoherent, still display relatively well defined Bloch character with pronounced momentum dispersion, see, e.g., Ref.[4]. As a matter of fact, it is often difficult to experimentally even distinguish the Hubbard bands found in Mott insulators from ordinary Bloch bands found at high energy in conventional band insulators. While such behavior can be already numerically reproduced by some modern many-body approximations[5,6], a simple conceptual picture for the apparent Bloch character of such high energy charge excitations is not still available. In particular, variational methods such as the Gutzwiller Approximation (GA)[7] — which are often able to reproduce the numerical results in a much simpler semi-analytical fashion — generally capture only the low-lying QP features on the metallic side, but cannot provide a description of charge excitations around the Mott point and in the insulating regime.

The goal of this Rapid Communication is to write an appropriate variational wave function able to capture the main features of both the (low energy) QP bands and the (high energy) Hubbard bands, within the same theoretical framework. A particularly interesting fact emerging from our theory is that many key attributes of both types of excitations are encoded in the bare density of states (DOS) of the uncorrelated system and a few renormalization parameters — in a similar fashion as for the QP excitations in Landau theory of Fermi liquids. This is accomplished, similarly as in many other theories for many-body systems, see, e.g., Refs.[8–10], by enlarging the Hilbert space by introducing auxiliary "ghost" degrees of freedom. In particular, this construction sheds light on the physical origin of the "hidden" Bloch character of the Hubbard bands mentioned above. Our calculations of the single-band Hubbard model, which are benchmarked against the Dynamical Mean Field Theory (DMFT)[5,6] solution, show that the new wave function quantitatively captures not only the dispersion of the QP but also of the Hubbard bands. Furthermore, our theory enables us to describe the Mott transition and the coexistence region between the metallic and the Mott-insulator phases.

Ghost GA theory:— For simplicity, our theory will be formulated here for the single-band Hubbard model

$$\hat{H} = \sum_{RR'} \sum_{\sigma} t_{RR'}\, c^{\dagger}_{R\sigma} c_{R'\sigma} + \sum_{R\sigma} U\, \hat{n}_{R\uparrow} \hat{n}_{R\downarrow} \qquad (1)$$

at half-filling. The generalization to arbitrary multi-orbital Hubbard Hamiltonians is straightforward[11].

In order to construct the Ghost-GA theory we are going to embed the physical Hamiltonian of the system [Eq. (1)] within an extended Hilbert space obtained by introducing auxiliary Fermionic "ghost" degrees of freedom *not* coupled with the physical orbitals, see Fig. 1. Let us represent $\hat{H}$ within the extended Hilbert space

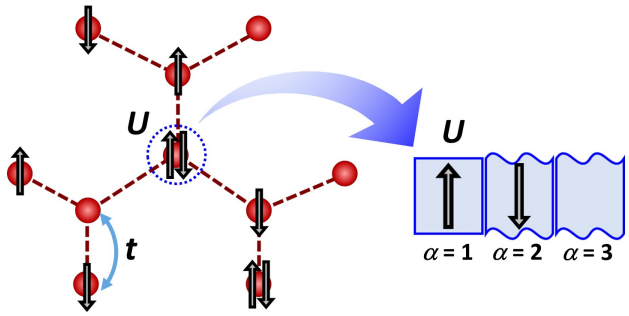

Figure 1: (Color online) Representation of a lattice including 2 ghost orbitals ($\alpha = 2, 3$). The Hamiltonian of the system acts as 0 over the the auxiliary ghost degrees of freedom. The Hubbard interaction U acts only on the physical orbital $\alpha = 1$.

mentioned above as follows:

$$\begin{aligned}\hat{H} &= \sum_{RR'}\sum_{\alpha\beta\sigma} \tilde{t}^{\alpha\beta}_{RR'}\, c^{\dagger}_{R\alpha\sigma} c_{R'\beta\sigma} + \sum_{R} U\, \hat{n}_{R1\uparrow}\hat{n}_{R1\downarrow} \\ &= \sum_{k}\sum_{\alpha\beta\sigma} \tilde{\epsilon}^{\alpha\beta}_{k}\, c^{\dagger}_{k\alpha\sigma} c_{k\beta\sigma} + \sum_{R} U\, \hat{n}_{R1\uparrow}\hat{n}_{R1\downarrow}\,, \end{aligned} \tag{2}$$

where $\tilde{t}^{11}_{RR'} = t_{RR'}$ are the physical hopping parameters, $\tilde{\epsilon}^{11}_{k} = \epsilon_k$ are the eigenvalues of the first term of $\hat{H}$, $\tilde{t}^{\alpha\beta}_{RR'} = \tilde{\epsilon}^{\alpha\beta}_{k} = 0\ \forall\,(\alpha,\beta) \neq (1,1)$ and σ is the spin.

Our theory consists in applying the ordinary multi-orbital GA theory[14–18] to Eq (2). In other words, the expectation value of $\hat{H}$ is optimized variationally with respect to a Gutzwiller wave function represented as $|\Psi_G\rangle = \hat{\mathcal{P}}_G|\Psi_0\rangle$, where $|\Psi_0\rangle$ is the most general Slater determinant, $\hat{\mathcal{P}}_G = \prod_R \hat{\mathcal{P}}_R$, and $\hat{\mathcal{P}}_R$ acts over all of the local degrees of freedom labeled by R — including the ghost orbitals $\alpha > 1$ — and commutes with the total number operator $\sum_{\alpha\sigma} c^{\dagger}_{R\alpha\sigma} c_{R\alpha\sigma}$. The variational wave function is restricted by the following conditions:

$$\langle\Psi_0|\,\hat{\mathcal{P}}^{\dagger}_R\hat{\mathcal{P}}_R\,|\Psi_0\rangle \;=\; \langle\Psi_0|\Psi_0\rangle \tag{3}$$

$$\langle\Psi_0|\,\hat{\mathcal{P}}^{\dagger}_R\hat{\mathcal{P}}_R\, c^{\dagger}_{R\alpha\sigma}c_{R\beta\sigma}\,|\Psi_0\rangle \;=\; \langle\Psi_0|\,c^{\dagger}_{R\alpha\sigma}c_{R\beta\sigma}\,|\Psi_0\rangle\,, \tag{4}$$

which are commonly called "Gutzwiller constraints". Furthermore, the so called "Gutzwiller Approximation"[7] — which is exact in the limit of infinite dimensions (where DMFT is exact) — is employed. The minimization of the variational energy will be performed by employing the algorithms derived in Ref.[19].

Note that extending the Hilbert space by introducing the ghost orbitals does not affect the physical Hubbard Hamiltonian $\hat{H}$, as all of its terms involving ghost orbitals are multiplied by 0, see Eq. (2).

The advantage of enlarging the Hilbert space arises from the fact that the resulting Ghost-GA variational wavefunction is substantially richer with respect to the ordinary GA[11]. In particular, $|\Psi_0\rangle$ is variationally allowed to be any multi-orbital Slater determinant lying within the the whole extended Hilbert space, i.e., to display entanglement between physical and auxiliary degrees of freedom. However, as proven explicitly in the supplemental material[11], the Gutzwiller local operator $\hat{\mathcal{P}}_G = \prod_R \hat{\mathcal{P}}_R$, which is also variationally determined, maps $|\Psi_0\rangle$ into a *physical* correlated wavefunction $|\Psi_G\rangle = \hat{\mathcal{P}}_G|\Psi_0\rangle$, i.e., into a many-body state disentangled from the auxiliary ghost space (consistently with the fact that $\hat{H}$ depends exclusively on the physical degrees of freedom). Thus, the benefit of enlarging the Hilbert space is that it enables us to extend the ordinary GA variational space, while retaining the mathematical structure of the conventional GA theory.

We point out that the Ghost-GA variational construction outlined above presents insightful formal and physical analogies with the theories of Matrix Product States (MPS) and Projected Entangled Pair States (PEPS)[9,10], which are also variational schemes involving *virtual* entanglement and local maps from an auxiliary extended Hilbert space into the physical space[20].

Excitations:— As shown in previous works, see, e.g., Refs.[16], the variational energy minimum of $\hat{H}$ is realized by a wave function $|\Psi_G\rangle = \hat{\mathcal{P}}_G|\Psi_0\rangle$ where $|\Psi_0\rangle$ is the ground state of a quadratic multi band Hamiltonian represented as

$$\hat{H}_{\rm qp} = \sum_{kab\sigma} \left[\tilde{\mathcal{R}}\tilde{\epsilon}_k\tilde{\mathcal{R}}^{\dagger} + \tilde{\lambda}\right]_{ab} f^{\dagger}_{ka\sigma} f_{kb\sigma} = \sum_{kn\sigma} \tilde{\epsilon}^{*}_{kn}\psi^{\dagger}_{kn\sigma}\psi_{kn\sigma}, \tag{5}$$

where $f_{ka\sigma}$ are related to $c_{ka\sigma}$ by a proper unitary transformation[14,16], the matrices $\tilde{\mathcal{R}}$ and $\tilde{\lambda}$ are determined variationally, and $\tilde{\epsilon}^{*}_{kn}$ and $\psi^{\dagger}_{ka\sigma}$ are the eigenvalues and eigenoperators of $\hat{H}_{\rm qp}$, respectively. The states $|\Psi^{p}_{Gkn\sigma}\rangle = \hat{\mathcal{P}}_G\psi^{\dagger}_{kn\sigma}|\Psi_0\rangle$ and $|\Psi^{h}_{Gkn\sigma}\rangle = \hat{\mathcal{P}}_G\psi_{kn\sigma}|\Psi_0\rangle$ represent excited states of $\hat{H}$[11,21,22].

The energy-resolved Green's function of the physical degrees of freedom ($\alpha = 1$) can be evaluated in terms of the excitations mentioned above[11] and represented as

$$G(\epsilon_k,\omega) = \left[\tilde{\mathcal{R}}^{\dagger}\frac{1}{\omega - \left(\tilde{\mathcal{R}}\tilde{\epsilon}_k\tilde{\mathcal{R}}^{\dagger} + \tilde{\lambda}\right)}\tilde{\mathcal{R}}\right]_{11} = \left[\omega - \epsilon_k - \Sigma(\omega)\right]^{-1}, \tag{6}$$

where the subscript "11" indicates that we are interested only in the physical component $\alpha = \beta = 1$ of the Green's function. As we are going to see, the Ghost-GA approximation to the physical self-energy $\Sigma(\omega)$, see Eq. (6), is generally a *non-linear* function of ω[11,23,24] — while it is linear by construction within the ordinary GA theory. Note also that the poles of $G(\epsilon_k,\omega)$ coincide with the eigenvalues $\tilde{\epsilon}^{*}_{kn}$ of $\hat{H}_{\rm qp}$, see Eqs. (5) and (6).

Application to the single-band Hubbard model:— Below we apply our approach to the Hubbard Hamiltonian [Eq. (2)] at half-filling assuming a semicircular DOS[25], which corresponds, e.g., to the Bethe lattice in the limit of infinite connectivity, where DMFT is exact[5]. The half-bandwidth D will be used as the unit of energy. The extended Ghost-GA scheme will be applied following the procedure of Ref.[19], utilizing up to 2 ghost orbitals.

In Fig. 2 is shown the evolution as a function of the Hubbard interaction strength U of the Ghost-GA total energy, the local double occupancy and the QP weight z. Our results are shown in comparison with the ordinary GA theory and with DMFT in combination with Numerical Renormalization Group (NRG). In particular, we employed the "NRG Ljubljana" impurity solver[26].

The agreement between Ghost-GA and DMFT is quantitatively remarkable. In particular, the Ghost-GA theory enables us to account for the coexistence region of the Mott and metallic phases, which is not captured by the ordinary GA theory. The values of the boundaries of the coexistence region $U_{c1} \simeq 2$, $U_{c2} \simeq 2.88$ are in good agreement with the DMFT results available in the literature[27–30], i.e., $U_{c1} \simeq 2.39$, $U_{c2} \simeq 2.94$. The Ghost-GA value of U_{c2}, which is the actual Mott transition point at $T = 0$, is particularly accurate. The method also gives a reasonable value for the very small energy scale characterizing the coexistence region, which we can estimate as $T_c \simeq E_{\rm ins}(U_{c1}) - E_{\rm met}(U_{c1}) \simeq 0.02$, consistently with both DMFT and experiments[31,32]. We point out also that, as shown in the second panel of Fig. 2, the Ghost-GA approach captures the charge fluctuations in the Mott phase, while this is approximated by the simple atomic limit (which has zero double occupancy) within the Brinkman-Rice scenario[33].

Interestingly, while at least 2 ghost orbitals are necessary to obtain the data illustrated above for the Metallic solution, 1 ghost orbital is sufficient to obtain our results concerning the Mott phase. Increasing further the number of ghost orbitals does not lead to any appreciable difference[11]. As we are going to show, this is connected with the fact that the electronic structures of the Mott and the metallic phases are topologically distinct.

Let us now analyze the Ghost-GA single-particle Green's function $G(\epsilon,\omega)$, see Eq. (6). In Fig. 3 is shown the Ghost-GA energy-resolved spectral function $A(\epsilon,\omega) = -\frac{1}{\pi}{\rm Im}G(\epsilon,\omega)$ in comparison with DMFT[34]. Although the broadening of the bands (scattering rate), is not captured by our approximation (as it is not captured by the ordinary GA), the positions and the weights of the poles of the Ghost-GA spectral function encode most of the DMFT features, not only at low energies (QP excitations), but also at high energies (Hubbard bands). In order to analyze how the spectral properties of the system emerge within the Ghost-GA theory, it is particularly convenient to express the QP Hamiltonian [Eq. (5)] in a gauge where $\tilde{\lambda}$ is diagonal[35].

In the metallic phase, an explicit Ghost-GA calculation obtained employing 2 ghost orbitals shows that the matrices $\tilde{\mathcal{R}}$ and $\tilde{\lambda}$ are represented as follows:

$$\tilde{\lambda}_{ij} \;=\; l\,\delta_{ij}(\delta_{2i}-\delta_{3i}) \qquad (7)$$

$$\tilde{\mathcal{R}}_{ij} \;=\; \delta_{j1}\left(\sqrt{z}\,\delta_{i1}+\sqrt{h}\,(\delta_{i2}+\delta_{i3})/\sqrt{2}\right)\,, \qquad (8)$$

where δ_{ij} is the Kronecker delta, and l, z and h are real positive numbers determined numerically as in Ref.[19].

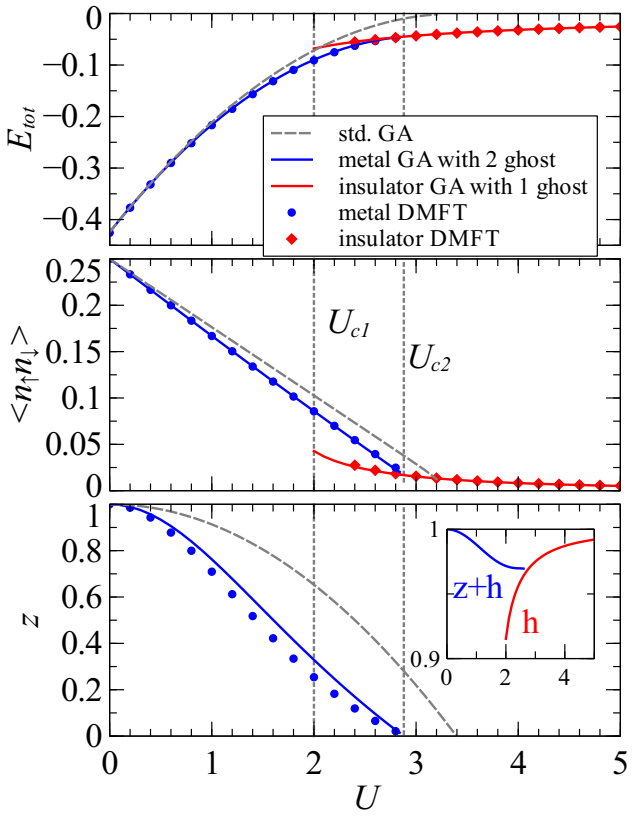

Figure 2: (Color online) Evolution of total energy (upper panel), local double occupancy (middle panel) and QP weight (lower panel) as a function of the Hubbard interaction strength U for the single-band Hubbard model with semicircular DOS at half-filling. The Ghost-GA results are shown in comparison with the ordinary GA and with DMFT+NRG. The Ghost-GA boundaries of the coexistence region U_{c1}, U_{c2} are indicated by vertical dotted lines. Inset: Integral of Ghost-GA local spectral weight over all frequencies (see discussion in main text).

The corresponding self-energy, see Eq. (6), is[36]:

$$\Sigma(\omega) = \frac{\omega}{1+\frac{1}{z-\frac{\omega^2-l^2+2h\omega^2}{\omega^2-l^2}}} = -\frac{1-z}{z}\,\omega + o(\omega^2)\,. \qquad (9)$$

Thus, the variational parameter z of Eq. (8) represents the QP weight, whose behavior was displayed in the third panel of Fig. 2. Note that the overall spectral weight $\int d\omega \int d\epsilon\, \rho(\epsilon)\, A(\epsilon,\omega)$, where $\rho(\epsilon)$ is the semicircular DOS, is not z as in the ordinary GA theory, but it is $z+h = [\tilde{\mathcal{R}}^\dagger\tilde{\mathcal{R}}]_{11}$, which is almost equal to 1 for all values of U (see the inset of the third panel in Fig. 2). The additional spectral contribution h, which is not present in the ordinary GA approximation, enables the Ghost-GA theory to account for the Hubbard bands.

In the Mott phase, an explicit Ghost-GA calculation obtained employing 1 ghost orbital shows that the matrices $\tilde{\mathcal{R}}$ and $\tilde{\lambda}$ are represented as follows:

$$\tilde{\lambda}_{ij} \;=\; l\,\delta_{ij}(\delta_{1i}-\delta_{2i}) \qquad (10)$$

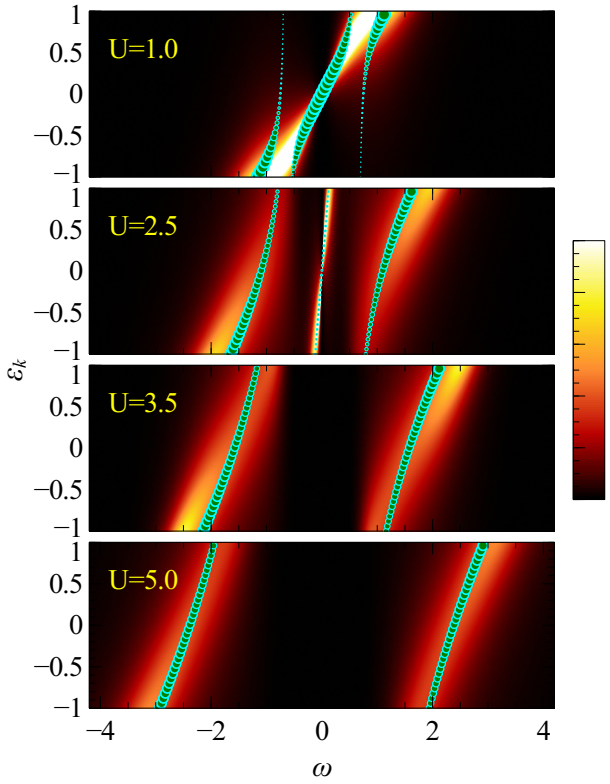

Figure 3: (Color online) Poles of the Ghost-GA energy-resolved Green's function (bullets), see Eq. (6), in comparison with DMFT+NRG. The size of the bullets indicates the spectral weights of the corresponding poles. Metallic solution for $U = 1$, 2.5 and Mott solution for $U = 3.5$, 5.

$$\tilde{\mathcal{R}}_{ij} \;=\; \delta_{j1}\sqrt{h}\,(\delta_{i1}+\delta_{i2})/\sqrt{2}\,, \qquad (11)$$

where l and h are real positive numbers determined numerically as in Ref. 19. Note that $h = [\tilde{\mathcal{R}}^\dagger\tilde{\mathcal{R}}]_{11} \simeq 1$ (see the inset of the third panel in Fig. 2). The corresponding self-energy, see Eq. (6), is[36]:

$$\Sigma(\omega) = -\frac{1-h}{h}\,\omega + \frac{l^2}{h}\,\frac{1}{\omega}\,. \qquad (12)$$

The pole of the self energy at $\omega = 0$, which is the source of the Mott gap, is captured by the Ghost-GA theory.

The analysis above clarifies also why, by construction, within the Ghost-GA approximation the self-energy can develop poles, see Eqs. (9) and (12), but can not capture branch-cut singularities on the real axis.

We point out that enlarging the Hilbert space has been essential in order to capture the effect of the electron correlations on the topology of the excitations — such as the change of the number of bands at the Mott transition (between 3 bands in the metallic phase and 2 bands in the Mott phase). In fact, without extending the Hilbert space, the ordinary GA theory enables only to renormalize and shift the band structure with respect to the uncorrelated limit $U = 0$, without affecting its qualitative topological structure. On the other hand, extending the Hilbert space enables us to relax this constraint, as $G(\epsilon, \omega)$, see Eq. (6), is variationally allowed to have any number of distinct poles equal or smaller to the corresponding total (physical and ghost) number of orbitals[11]. It is for this reasons that only 1 ghost (2 orbitals) is sufficient to describe the Mott phase of the single-band Hubbard model, while at least 2 ghosts (3 orbitals) are necessary in order to describe its metallic phase — whose spectra includes the QP excitations and the 2 Hubbard bands. A remarkable aspect of this construction is that, within the Ghost-GA theory, the information concerning the spectral function — including the Hubbard bands — is entirely encoded in only 3 parameters (z, h, l) in the Metallic phase, and in 2 parameters (h, l) in the Mott phase, see Eqs. (7), (8), (10), (11).

Conclusions:— We derived a unified theoretical picture for excitations in Mott systems based on a generalization of the GA, which captures not only the low-energy QP excitations, but also the Hubbard bands. The key idea consists in enlarging the Hilbert space of the system by introducing auxiliary "ghost" orbitals. This construction enables us to express analytically many important features of both types of excitations in terms of the bare DOS of the uncorrelated system and a few renormalization parameters, in a similar fashion as for the QP excitations in Landau theory of Fermi liquids. In particular, this provides us with a conceptual picture which assigns naturally a Bloch character to the Hubbard bands even in Mott insulators. In this respect, we note that our theory presents a few suggestive analogies with the interesting idea of "hidden Fermi liquid", previously introduced by P. W. Anderson[37] within the context of the BCS wave function (for superconductors) and the Laughlin's Jastrow wave function (for the Fractional Hall Effect). In fact, they both propose a descriptions of non-Fermi liquid states related to ordinary Fermi liquids residing in unphysical Hilbert spaces, see, e.g., Ref.[38]. From the computational perspective, the Ghost-GA theory constitutes a very promising tool for ab-initio calculations in combination with Density Functional Theory[16,18,39–41], as it is substantially more accurate with respect to the ordinary GA approximation, without much additional computational cost. In fact, within the numerical scheme described in Refs.[16,19], our theory results in solving iteratively a finite impurity model, where the number of bath sites grows linearly with the total number of ghost orbitals[11]. Since there exist numerous available techniques enabling to solve efficiently this auxiliary problem, see, e.g., Refs.[42–46], this work opens an exciting avenue for realistic modeling of many challenging materials, including predictions of ARPES spectra for complex orbitally-selective Mott insulators and "materials by design" of strongly correlated electron systems. Furthermore, since the Ghost-GA theory is based on the multi-orbital GA[16,19], it can be straightforwardly generalized to finite temperatures[47–49], to non-equilibrium problems[50,51], and to calculate linear response functions[52]. For the same reason, the Ghost-

GA theory can be reformulated[14,16,53] in terms of the rotationally invariant slave boson (RISB) theory[11,54,55], whose exact operatorial foundation recently derived in Ref.[19] constitutes a starting point to calculate further corrections[56]. It would be also interesting to apply the ghost-orbital Hilbert space extension in combination with the Variational Monte Carlo method[57] or the generalization of the GA to finite dimensions of Ref.[58], which might lead to a more accurate description of strongly correlated electron systems, even beyond the DMFT approximation.

Acknowledgments

N.L., T.H. and V.D. were partially supported by the NSF grant DMR-1410132 and the National High Magnetic Field Laboratory. Y.Y. was supported by the U.S. Department of energy, Office of Science, Basic Energy Sciences, as a part of the Computational Materials Science Program.

[1] L. D. Landau, Soviet Physics JETP **3**, 920 (1957).
[2] A. Damascelli, Physica Scripta **T109**, 61 (2004).
[3] G. Binnig, H. Rohrer, C. Gerber, and E. Weibel, Phys. Rev. Lett. **49**, 57 (1982).
[4] D. V. Evtushinsky, M. Aichhorn, Y. Sassa, Z.-H. Liu, J. Maletz, T. Wolf, A. N. Yaresko, S. Biermann, S. V. Borisenko, and B. Buchner (2017), cond-mat/1612.02313.
[5] A. Georges, G. Kotliar, W. Krauth, and M. J. Rozenberg, Rev. Mod. Phys. **68**, 13 (1996).
[6] V. Anisimov and Y. Izyumov, *Electronic Structure of Strongly Correlated Materials* (Springer, 2010).
[7] M. C. Gutzwiller, Phys. Rev. **137**, A1726 (1965).
[8] I. Affleck, T. Kennedy, E. H. Lieb, and H. Tasaki, Phys. Rev. Lett. **59**, 799 (1987).
[9] F. Vaestrate, J. Cirac, and V. Murg, Adv. Phys. **57**, 143 (2008).
[10] U. Schollwock, Annals of Physics **96**, 326 (2011).
[11] Supplemental material: Technical details and Ghost-GA calculations using more ghost orbitals, which includes Refs. [12,13].
[12] A. C. Hewson, *The Kondo Problem to Heavy Fermions* (Cambridge University Press, 1997).
[13] N. Lanatà, Phys. Rev. B **82**, 195326 (2010).
[14] N. Lanatà, P. Barone, and M. Fabrizio, Phys. Rev. B **78**, 155127 (2008).
[15] J. Bünemann, W. Weber, and F. Gebhard, Phys. Rev. B **57**, 6896 (1998).
[16] N. Lanatà, Y. Yao, C.-Z. Wang, K.-M. Ho, and G. Kotliar, Phys. Rev. X **5**, 011008 (2015).
[17] C. Attaccalite and M. Fabrizio, Phys. Rev. B **68**, 155117 (2003).
[18] X.-Y. Deng, L. Wang, X. Dai, and Z. Fang, Phys. Rev. B **79**, 075114 (2009).
[19] N. Lanatà, Y. Yao, X. Deng, V. Dobrosavljević, and G. Kotliar, Phys. Rev. Lett. **118**, 126401 (2017).
[20] Note also that, as the MPS, the Ghost-GA wavefunction does not break artificially the translational invariance of the system.
[21] J. Bünemann, F. Gebhard, and R. Thul, Phys. Rev. B **67**, 075103 (2003).
[22] N. Lanatà, Ph.D. thesis, SISSA-Trieste (2009).
[23] S. Y. Savrasov, K. Haule, and G. Kotliar, Phys. Rev. Lett. **96**, 036404 (2006).
[24] S. Y. Savrasov, V. Oudovenko, K. Haule, D. Villani, and G. Kotliar, Phys. Rev. B **71**, 115117 (2005).
[25] Our results do not qualitatively depend on the specific choice of DOS.
[26] R. Zitko, Comp. Phys. Comm. **182**, 2259 (2011).
[27] D. J. García, K. Hallberg, and M. J. Rozenberg, Phys. Rev. Lett. **93**, 246403 (2004).
[28] P. Werner and A. J. Millis, Phys. Rev. B **75**, 085108 (2007).
[29] R. Bulla, Phys. Rev. Lett. **83**, 136 (1999).
[30] N.-H. Tong, S.-Q. Shen, and F.-C. Pu, Phys. Rev. B **64**, 235109 (2001).
[31] M. C. O. Aguiar, V. Dobrosavljević, E. Abrahams, and G. Kotliar, Phys. Rev. B **71**, 205115 (2005).
[32] P. Limelette, P. Wzietek, S. Florens, A. Georges, T. A. Costi, C. Pasquier, D. Jérome, C. Mézière, and P. Batail, Phys. Rev. Lett. **91**, 016401 (2003).
[33] W. F. Brinkman and T. M. Rice, Phys. Rev. B **2**, 4302 (1970).
[34] M. Karski, C. Raas, and G. S. Uhrig, Phys. Rev. B **77**, 075116 (2008).
[35] Eq. (6) is invariant with respect to any gauge transformation $\tilde{\mathcal{R}} \to u^\dagger \tilde{\mathcal{R}}$, $\tilde{\lambda} \to u^\dagger \tilde{\lambda} u$, where u is unitary, see Ref.[19].
[36] Note that the expression for $\Sigma(\omega)$ is k indepenent as expected, since we employed the GA.
[37] P. W. Anderson, Phys. Rev. B **78**, 174505 (2008).
[38] J. K. Jain and P. W. Anderson, Proc. Nat. Acad. Sci. **106**, 9131 (2009).
[39] P. Hohenberg and W. Kohn, Phys. Rev. **136**, B864 (1964).
[40] W. Kohn and L. J. Sham, Phys. Rev. **140**, A1133 (1965).
[41] K. M. Ho, J. Schmalian, and C. Z. Wang, Phys. Rev. B **77**, 073101 (2008).
[42] F. A. Wolf, A. Go, I. P. McCulloch, A. J. Millis, and U. Schollwöck, Phys. Rev. X **5**, 041032 (2015).
[43] H. Saberi, A. Weichselbaum, and J. von Delft, Phys. Rev. B **78**, 035124 (2008).
[44] A. Weichselbaum, F. Verstraete, U. Schollwöck, J. I. Cirac, and J. von Delft, Phys. Rev. B **80**, 165117 (2009).
[45] Y. Lu, M. Höppner, O. Gunnarsson, and M. W. Haverkort, Phys. Rev. B **90**, 085102 (2014).
[46] N. Lanatà, Y.-X. Yao, X. Deng, C.-Z. Wang, K.-M. Ho, and G. Kotliar, Phys. Rev. B **93**, 045103 (2016).
[47] N. Lanatà, X.-Y. Deng, and G. Kotliar, Phys. Rev. B **92**, 081108 (2015).
[48] M. Sandri, M. Capone, and M. Fabrizio, Phys. Rev. B **87**, 205108 (2013).
[49] W.-S. Wang, X.-M. He, D. Wang, Q.-H. Wang, Z. D. Wang, and F. C. Zhang, Phys. Rev. B **82**, 125105 (2010).
[50] M. Schirò and M. Fabrizio, Phys. Rev. Lett. **105**, 076401 (2010).
[51] N. Lanatà and H. U. R. Strand, Phys. Rev. B **86**, 115310 (2012).
[52] M. Fabrizio, Phys. Rev. B **95**, 075156 (2017).
[53] J. Bünemann and F. Gebhard, Phys. Rev. B **76**, 193104 (2007).

[54] F. Lechermann, A. Georges, G. Kotliar, and O. Parcollet, Phys. Rev. B **76**, 155102 (2007).
[55] T. Li, P. Wölfle, and P. J. Hirschfeld, Phys. Rev. B **40**, 6817 (1989).
[56] V. H. Dao and R. Frésard, Phys. Rev. B **95**, 165127 (2017).
[57] D. Ceperley, G. V. Chester, and M. H. Kalos, Phys. Rev. B **16**, 3081 (1977).
[58] K. z. Münster and J. Bünemann, Phys. Rev. B **94**, 045135 (2016).